

# Sector and Site Switch-Off Regular Patterns for Energy Saving in Cellular Networks

Tamer Beitelmal<sup>1</sup>, Sebastian S. Szyszkowicz<sup>2</sup>, *Member, IEEE*, David González G.<sup>3</sup>, *Member, IEEE*,  
and Halim Yanikomeroglu<sup>4</sup>, *Fellow, IEEE*

**Abstract**—Cell switch-off (CSO) is an important approach to reducing energy consumption in cellular networks during off-peak periods. CSO addresses the research question of which cells to switch off when. Whereas *online* CSO, based on immediate user demands and channel states, is problematic to implement and difficult to model, *off-line* CSO is more practical and tractable. Furthermore, it is known that regular cell layouts generally provide the best coverage and spectral efficiency, which leads us to prefer regular static (off-line) CSO. We introduce sector-based regular CSO patterns for the first time. We organize the existing and newly introduced patterns using a systematic nomenclature; studying 26 patterns in total. We compare these patterns in terms of energy efficiency and the average number of users supported, via a combination of analysis and simulation. We also compare the performance of CSO with two benchmark algorithms. We show that the average number of users can be captured by one parameter. Moreover, we find that the distribution of the number of users is close to Gaussian, with a tractable variance. Our results demonstrate that several patterns that activate only one out of three sectors are particularly beneficial; such CSO patterns have not been studied before.

**Index Terms**—Cell switch-off (CSO), green cellular networks, offline CSO, renewal processes, sector-based CSO.

## I. INTRODUCTION

FIFTH generation (5G) wireless networks are expected to support up to 1,000-fold gains in capacity. Several sophisticated techniques are to be employed to achieve this ambitious target. A key enabler is network densification, installing more small cells, which can be seen as bringing the network closer to the user equipment (UE) in order to improve its received power [2]. On top of network densification, aggressive frequency reuse is adopted to efficiently utilize the

scarce spectrum. Although promising to achieve higher rates, installing more cells results in higher energy consumption. This is because base stations (BSs) consume 50-80% of the total energy in a cellular network [3], [4]. Energy consumption of a cell is not proportional to its load level, i.e., a lightly loaded cell consumes approximately the same energy as a fully loaded one [5], [6].

This increase in energy consumption conflicts with the energy efficiency targets of 5G networks. An effective approach to meeting these targets is to switch off some cells entirely in periods of low traffic and distribute their UEs to nearby cells. This approach, known as cell switch-off (CSO), aims to reduce energy consumption without sacrificing the quality of service (QoS) or the coverage area. Although relatively new, several CSO schemes have been proposed to tackle the issues from different angles (see survey papers [7], [8] for details).

One important issue in CSO is interference modelling, which is challenging because it is hard to know the set of active cells a priori. Typically, UEs are connected to the best cell/sector in terms of downlink signal-to-interference-plus-noise ratio (SINR). However, when switching off a sector, its UEs need to be reassigned to another, perhaps less advantageous, sector. Without a proper interference characterization, these UEs might encounter a large amount of interference because the set of active cells that contribute to the interference is only known at the final stage. The predicted performance is hence inaccurate. Indeed, some CSO approaches assume zero interference, i.e., there is a perfect inter-cell interference coordination (ICIC) [5], [9]. This assumption is too optimistic and produces an unachievable upper bound on the number of switched-off cells. Other approaches model interference by assuming that all cells fully contribute to the interference, as if they were active all the time [10]. This assumption yields a poor lower bound on the number of switched-off cells.

One accurate way to model interference, thus alleviating the aforementioned problem, is by predetermining the set of active cells, i.e., the cells that actually generate the interference in the system. This is sometimes referred to as offline or static CSO [7], [8]. It is possible to predetermine several configurations of active cells for different traffic densities and then select an appropriate configuration to accommodate the specific demand distribution.

Regular static CSO (CSO patterns) is a special case of static CSO, in which active BSs are predetermined such that

Manuscript received October 11, 2016; revised April 7, 2017 and October 31, 2017; accepted January 24, 2018. Date of publication February 13, 2018; date of current version May 8, 2018. This work was supported in part by the TELUS Corporation and in part by the Ministry of Higher Education and Scientific Research, Libya, through the Libyan-North American Scholarship Program. This paper was presented at the IEEE Vehicular Technology Conference, September 2016 [1]. The associate editor coordinating the review of this paper and approving it for publication was R. Hu. (*Corresponding author: Tamer Beitelmal.*)

T. Beitelmal, S. S. Szyszkowicz, and H. Yanikomeroglu are with the Department of Systems and Computer Engineering, Carleton University, Ottawa, ON K1S 5B6, Canada (e-mail: tamer@sce.carleton.ca; sz@sce.carleton.ca; halim@sce.carleton.ca).

D. González G. is with the Department of Communications and Networking, Aalto University, 02150 Espoo, Finland (e-mail: david.gonzalez.g@ieee.org).

Color versions of one or more of the figures in this paper are available online at <http://ieeexplore.ieee.org>.

Digital Object Identifier 10.1109/TWC.2018.2804397

their locations form a cellular layout that is as regular as possible [8]. If we think of a *pattern* as the configuration of active sectors, then in *regular CSO patterns* the locations of active cells form a regular layout (configuration) that is repeated in a spatially periodic manner. It has been shown that, for the same number of BSs, the best SINR distribution can be achieved when the BSs are located on a regular grid [11]. Therefore, CSO patterns were introduced in the literature to make the interference tractable and jointly avoid coverage holes. The possibility of successfully adopting regular CSO patterns is investigated in this paper; our results positively confirm this hypothesis and also show that switching off individual sectors results in better performance. This paper focuses mainly on networks with dense cell deployments with short inter-site distances. In such a deployment, the uplink coverage is not as significant as the downlink.

Regular CSO patterns are based on a logical-AND combination of site-level and sector-level patterns. We compare the performances of these patterns in terms of number of UEs supported, downlink SINR distribution, and energy efficiency, and also provide an illustrative case study. In most cases, patterns in which one out of three sectors is active (the same sector in each BS) can support the most UEs per sector, due to favourable interference positioning.

*Contributions:* The paper's contributions are summarized as follows:

- To the best of our knowledge, this paper is the first to introduce sector-based regular CSO patterns, where not only entire BSs could be switched off, but their individual sectors too. Note that switching off sectors individually is a common practice in online CSO literature.
- We analytically compare site-based versus sector-based CSO patterns in terms of energy efficiency. Because switching off one sector out of three per BS does not necessarily save one-third of the energy, we considered the power consumption of the common hardware shared between sectors of the same site.
- We compare the performance of different CSO patterns in terms of the number of supported users. We introduce a novel metric, the equivalent spectral efficiency (ESE): the mean performance of a given pattern can be captured using only this one metric, abstracting from the bandwidth and the rate. In this paper, we use a realistic and complex channel model [12], which makes the ESE analytically intractable; as such, we obtain the ESE values using simulation. We split the problem into analytical and simulation parts so that the methodology can be used for any channel model and link performance assumptions. We use these simulated values to obtain the distribution of the number of users analytically using the renewal process theory, which is a novel tool in this context. We illustrate this in detail with a case study.
- We organize the existing and the new CSO patterns using a systematic nomenclature.

This paper is organized as follows: Section II classifies the different CSO approaches. Section III provides the mathematical methodology, introduces different CSO patterns and analyses their energy efficiency. Section IV describes the

simulation setup, while Section V provides a comparative case study. Section VI concludes the paper.

## II. CSO CLASSIFICATIONS

There are two main CSO categories; online and offline. In the CSO literature, BSs are usually distributed on a regular grid – often triangular, sometimes square.<sup>1</sup> In the context of regular static CSO, sector-based CSO may offer additional opportunities for energy saving that have not been explored.

### A. Online CSO

In online CSO, an algorithm is executed in real time to determine the set of cells to be switched off. This requires global knowledge of the channel state information between each UE and each cell, as well as the load levels of all cells in the network. It is difficult for this vast amount of information to be exchanged by the network in a timely manner [7]. The computational time for the optimization might also be prohibitive for large-scale networks. Finally, some challenges in online CSO are: interference modelling due to the fact that the set of active cells is not known a priori and the time required for the on-off/off-on switching of BSs and for completing the handover procedures [15].

Online CSO is also known as *dynamic CSO* [8] and can be further classified as *fast-reaction* or *slow-reaction*.

1) *Fast-Reaction Online CSO:* The algorithms are supposed to adapt quickly to changes in the current user demand and attempt to provide optimal energy savings [16]. This category allows for a fast change in the network configuration (within a few seconds at most).

2) *Slow-Reaction Online CSO:* The change in network configuration requires a relatively longer time and only allows for long-term changes (within tens of seconds to minutes). These algorithms operate based on the average traffic measures or available traffic statistics, usually relying on certain traffic pattern recognition capabilities.

### B. Offline CSO

In offline CSO, different sets of active cells are predetermined offline, and the operator chooses the appropriate set to accommodate the current traffic density [17]. Only information related to the predetermined set of active cells is needed. Offline CSO is usually applicable for longer time scales (hours) and is often based on historical load distribution.

Offline CSO is also known as static CSO [8] and can be further classified as *static* or *regular static*.

1) *Static CSO:* Unlike online CSO, the network configuration in static CSO remains static for a long period of time. Therefore, the interference could be modelled appropriately (in statistical terms) by considering only the predetermined set of active cells [6]. Static CSO can be seen as a cell planning problem, but with constraints on BS locations; while in cell planning the cell placement is based on a wider set of possible locations, here the cell placement is restricted to the actual BS sites, from which a subset is chosen to be active.

<sup>1</sup>Recently, we have started exploring the CSO approach for spatially irregular BS deployments [13], [14].

TABLE I  
REGULAR CSO PATTERNS IN THE LITERATURE

Ref.	Site-level	Sector-level
[17]	$\frac{1}{4}$	Omni-directional
[20]	$\frac{2}{3}, \frac{2}{4}, \frac{3}{7}$	Omni-directional
[24]	$\frac{1}{2}$	Omni-directional
[25]	$\frac{1}{3}, \frac{1}{4}, \frac{1}{7}, \frac{1}{9}$	Omni-directional
[27]	$\frac{1}{3}, \frac{2}{3}, \frac{1}{4}, \frac{2}{4}, \frac{3}{4}$	Omni-directional
[26]	$\frac{1}{4}, \frac{1}{7}$	Omni-directional
[19]	$\frac{1}{4}, \frac{1}{7}, \frac{1}{9}$	$\frac{3}{3}$
[28]	$\frac{1}{4}, \frac{2}{4}, \frac{3}{4}$	$\frac{3}{3}$
This paper	$\frac{1}{3}, \frac{2}{3}, \frac{1}{4}, \frac{2}{4}, \frac{3}{4}, \frac{1}{7}, \frac{1}{9}$	$\frac{3}{3}, \frac{2}{3}, \frac{1}{3}$

2) *Regular CSO*: Regular CSO is a special case of static CSO, also known as *CSO patterns*. A *pattern* refers to the configuration of active sectors. Besides being predetermined offline, the set of active sectors is selected according to a periodic spatial pattern [8]. Regular CSO patterns resemble the intuitive and well-known frequency reuse<sup>2</sup> patterns [20].

In this paper, we propose regular CSO patterns as means to leverage the advantages of a regular topology (good SINR and coverage) [11]. By applying regular CSO, the choice of active cells minimizes coverage holes. This aspect is usually overlooked in the literature [21]. Also, regular CSO is more energy-efficient for UEs in the uplink, as there is always a nearby active cell [22], [23]. Regular CSO patterns reduce the interference between cells due to the careful selection of BS locations so that they are as far from each other as possible. The patterns are conceptually simple and can be described in a systematic way. Regular static CSO is useful when the user distribution is approximately uniform in space.

Regular CSO patterns are already under consideration by several research groups. The effect of different CSO patterns on the outage probability is investigated in [17] and [20], while the effect of the blocking probability is studied in [24]–[26]. Authors of [27] introduce a set of CSO patterns and propose a sophisticated OFDMA scheduler to jointly ensure full coverage for both downlink and uplink. Most papers consider omni-directional antennas (exceptions include [19], [28], yet focusing only on switching off the entire site.

Table I summarizes the existing literature on regular CSO patterns. The second column shows the site-level patterns (where the entire BS is switched off). The last column shows the sector-level patterns (where individual sectors are allowed to be switched off). In the last column, “omni-directional”

<sup>2</sup>Regular CSO patterns have conceptual similarities with frequency reuse. Here we can make a contrast with the performance of frequency reuse schemes, in which the average SINR increases with the frequency reuse factor [18, Table I]. This is because the distance to the nearest interfering BS is increased, while the cell size remains about the same. In regular static CSO, however, the cell grows with the decrease of the proportion of active sectors [19], which is analogous to the frequency reuse factor. The current practice in LTE is to employ a frequency reuse of one.

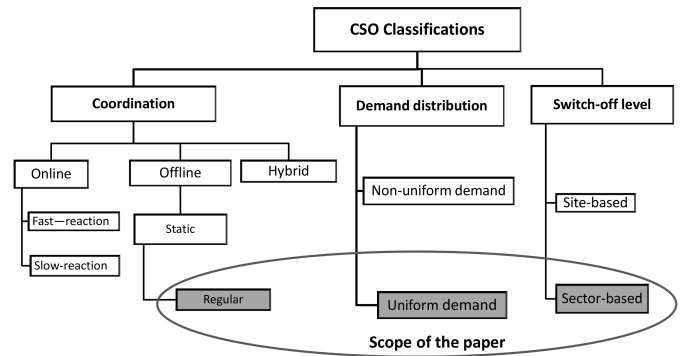


Fig. 1. Scope of the paper based on the CSO classifications.

indicates that the BS antennas are not sectorized, while the fractions “ $\frac{3}{3}$ ”, “ $\frac{2}{3}$ ” and “ $\frac{1}{3}$ ” indicate the number of active sectors per BS.

### C. Hybrid CSO

For better performance, it might be necessary to have a hybrid CSO approach where an online CSO algorithm is executed on top of the offline one. Starting with a static set of active cells to provide coverage and collect network information, the remaining cells participate in an online CSO algorithm to accommodate the fast variability in the traffic load [17]. Hybrid CSO is particularly useful when users are non-uniformly distributed in space.

### D. Switching Off Sectors

Most of the research in online CSO is executed in a sector-based manner, i.e., each sector can be turned off individually [6], [10]. However, to the best of our knowledge, this is not the case for regular CSO patterns, where only the entire BS (3 sectors) is turned off, i.e., no individual sector switch-off. We are the first to investigate sector-based regular CSO patterns.

In the rest of this paper, we show that regular CSO patterns with individual sector switch-off can be efficient in several interesting cases. In our simulation, each BS site has three 120°-sectors and the azimuth orientation of the sectors is the same for all sites.

### E. Scope of the Paper

This paper investigates regular CSO patterns, predetermined off-line, for the he meaningful and commonly used special case of uniform user distribution, where users are distributed according to Binomial point process (BPP). This paper introduces the sector-based regular CSO patterns for the first time, and organizes the existing and newly introduced patterns using a systematic nomenclature. As such, our work can be an intermediate step in studying CSO under more realistic (irregular BS locations and/or non-uniform user distribution) assumptions or it can be a be a part of more complex hybrid schemes. In order to further clarify the scope of this research we visually illustrated the scope of the paper in Fig. 1.

## III. METHODOLOGY

In this section, we explain the analysis for estimating the average number of supported users, introduce the two levels of

TABLE II  
LIST OF SYMBOLS FOR STATIC CSO PATTERNS

$W$	total system bandwidth
$N$	number of UEs that can be served per active sector
$\gamma_i$	SINR between UE $i$ and its serving sector
$\eta_i$	spectral efficiency of UE $i$ , = $\log_2(1 + \gamma_i)$ [bps/Hz]
$R_i$	rate required by UE $i$
$b_i$	bandwidth required by UE $i$ , = $R_i/\eta_i$ [Hz]
$\eta_{\text{eq}}$	equivalent spectral efficiency (ESE), = $1/\mathbb{E}\{1/\eta\}$ [bps/Hz/Sector]
$P_X(n/m, k/3)$	CSO pattern where $n$ out of $m$ BSs are active, $k$ out of 3 sectors are active, and $X$ is to distinguish between different rotations
$\rho$	proportion of active sectors in the network, = $ \mathbb{P}(n/m, k/3)  = \frac{nk}{3m} \in [0, 1]$
$P_{\text{site}}$	total power consumed at a fully active site
$P_{\text{pattern}}$	power consumed per system site for the selected pattern
$P_S$	power consumed per sector
$P_C$	common power consumed at a site
$\alpha$	= $P_C/P_S$ .
$\delta$	ratio of ESEs of two patterns
$P_o$	probability of signal outage (when $\gamma_i < -7$ dB)
$\text{CoV}\{X\}$	coefficient of variation of a random variable $X$ = $\sqrt{\text{Var}\{X\}}/\mathbb{E}\{X\}$

CSO patterns (site-level and sector-level), and then compare the sector-based versus site-based CSO patterns in terms of energy efficiency. The symbols used are provided in Table II.

The focus of this paper is to investigate and analyze the performance of regular CSO patterns during stable operation. Therefore, the user delay and other costs associated with BS switching are assumed to be similar for all CSO patterns. For details on the trade-off between the power consumption and the user delay, please see [29]. The intuition is that switching on/off BSs is a non-instantaneous process that involves several transitions which are not handled simultaneously. Also the time-scale of BS on-off/off-on switching is assumed to be larger than the time of the UE-to-BS association process.

#### A. Analysis of the Number of Supported Users

In this subsection, we study the distribution of the number  $N$  of UEs served by an active sector, and derive expressions for the mean number  $\mathbb{E}\{N\}$  of UEs, as well as for the distribution and variance of  $N$ . To do so, we introduce a novel metric to capture the mean performance of a given pattern. Due to the presence of several channel models and link performance assumptions, we split the problem into analytical and simulation parts, so that for a different channel model and link performance assumptions, all what is needed is to obtain the statistical values through simulation and then to apply the same method as mentioned below, i.e., there is no need to redo all the analysis all over again.

In our system, UEs are uniformly and independently distributed. The UE-to-cell assignment is such that UE  $i$  is connected to the sector that provides it with the best SINR  $\gamma_i$ . Hence, the spectral efficiency of UE  $i$  is calculated as

$$\eta_i = \log_2(1 + \gamma_i) \text{ [bps/Hz]}. \quad (1)$$

In CSO context, it is important to consider the outage probability  $P_o$ , in this paper the coverage percentage is equal

to  $(1 - P_o)$ . Some UEs might have a very weak SINR ( $< \gamma_{\min}$ ). When this happens, a UE cannot receive sufficiently strong signal for decoding and as a result will be in outage (considered when estimating the outage probability  $P_o$ ). Other UEs will have a very high SINR ( $> \gamma_{\max}$ ), to the extent that it might be higher than what the current constellations can utilize. As a result, these SINRs are truncated. For LTE networks, typical values for  $\gamma_{\min}$  and  $\gamma_{\max}$  are  $-7$  dB and  $18$  dB, respectively [30], [31].

To find the number of UEs  $N$  that can be served by an active sector, we formulate the problem as a renewal process (RP) [32, Ch. 7]. UEs are admitted to the network on a first-come, first-served basis. This is regardless of their bandwidth demand  $b_i$ , where

$$b_i = \frac{R_i}{\eta_i}, \quad (2)$$

which depends on the UE's downlink rate requirement  $R_i$ , and its downlink spectral efficiency  $\eta_i$ . At each sector, a newly arrived user  $i$  is assigned a portion of the bandwidth  $b_i$  such that its required rate  $R_i$  is satisfied. The assigned bandwidth is added up until the next UE's bandwidth  $b_{i+1}$  exceeds the sector's downlink bandwidth  $W$ . Thus we have

$$\sum_{i=1}^N b_i \leq W, \quad \text{and} \\ \sum_{i=1}^{N+1} b_i > W. \quad (3)$$

Since  $\{b_1, \dots, b_N, b_{N+1}\}$  is a sequence of positive independent and identically distributed (iid) random variables (RVs), the RP  $\bar{N}(w)$  is defined in terms of  $N$ ,  $b_i$ , and

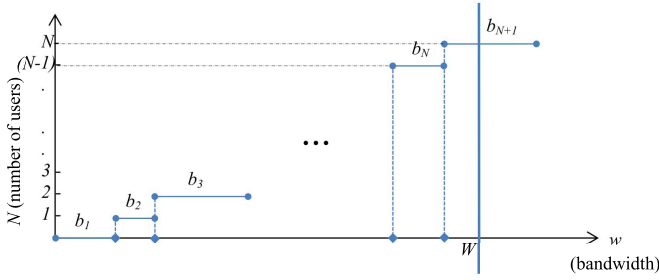


Fig. 2. A renewal process used to find the number of users  $N$  that can be supported by one sector with a bandwidth  $W$ , where  $b_i$  is the bandwidth required from UE  $i$  to satisfy its rate  $R_i$ .

a bandwidth  $w$  as

$$\bar{N}(w) = \max \left\{ N \in \mathbb{N} : \sum_i^N b_i \leq w \right\}. \quad (4)$$

Fig. 1 illustrates the RP, where UEs are admitted until there is no more bandwidth available at that sector for the next user UE $_{N+1}$ . If we consider  $W$  as the stopping time of this RP, we find that  $\bar{N}(W) = N$  is the number of UEs admitted by one active sector.

1) *Mean Number of Users:* From the Central Limit Theorem for RPs (RP-CLT)<sup>3</sup>: for large  $W$ , the distribution of  $\bar{N}(W)$  is approximately Gaussian [32, Ch. 7] with mean

$$\mathbb{E}\{N\} = W/\mathbb{E}\{b\}. \quad (5)$$

To find  $\mathbb{E}\{N\}$ , we first calculate  $\mathbb{E}\{b\}$  as

$$\mathbb{E}\{b\} = \mathbb{E}\left\{\frac{R}{\eta}\right\} = \mathbb{E}\{R\}\mathbb{E}\left\{\frac{1}{\eta}\right\}, \quad (6)$$

since  $R_i$  and  $\eta_i$  are independent RVs. Then, substituting  $\mathbb{E}\{b\}$  in (5),

$$\mathbb{E}\{N\} \cong \frac{W}{\mathbb{E}\{R\}}\eta_{\text{eq}}, \quad (7)$$

where we call  $\eta_{\text{eq}}$  the equivalent spectral efficiency (ESE), and is calculated as

$$\eta_{\text{eq}} = \frac{1}{\mathbb{E}\{1/\eta\}} \text{ [bps/Hz/Sector]}. \quad (8)$$

The ESE  $\eta_{\text{eq}}$  is an interesting metric, as it predicts the pattern performance abstracting from the bandwidth and the rate. The ESE is proportional to the mean number of supported users.

It is obtained by simulating many UEs in the network and considering their spectral efficiency.

2) *Variance and Distribution of Number of Users:* Similarly, again from the RP-CLT [32, Ch. 7], the variance of  $\bar{N}(W)$  is approximated by

$$\begin{aligned} \text{Var}\{N\} &\cong \frac{W \text{Var}\{b\}}{\mathbb{E}^3\{b\}} \\ &\cong \frac{W \text{Var}\{b\}}{\mathbb{E}^3\{R\}\mathbb{E}^3\{1/\eta\}}. \end{aligned} \quad (9)$$

<sup>3</sup>The RP-CLT for renewal processes is very different from the ordinary Central Limit Theorem (CLT): In the CLT, it is the sum of the RVs that is approximately Gaussian [32, Ch. 2], while in the RP-CLT, it is the number  $N$  of the summed RVs that is approximately Gaussian [32, Ch. 7].

First, we find  $\text{Var}\{b\}$  as

$$\begin{aligned} \text{Var}\{b\} &= \text{Var}\left\{\frac{R}{\eta}\right\} \\ &= \text{Var}\{R\}\text{Var}\left\{\frac{1}{\eta}\right\} \\ &\quad + \text{Var}\{R\}\mathbb{E}^2\left\{\frac{1}{\eta}\right\} \\ &\quad + \mathbb{E}^2\{R\}\text{Var}\left\{\frac{1}{\eta}\right\}. \end{aligned} \quad (10)$$

After plugging (10) into (9), and doing some simplifications, we obtain

$$\text{Var}\{N\} \cong \mathbb{E}\{N\}\text{CoV}^2\left\{\frac{1}{\eta}\right\} \times \left( \text{CoV}^2\{R\} + \frac{\text{CoV}\{R\}^2}{\text{CoV}^2\{1/\eta\}} + 1 \right), \quad (11)$$

where  $\text{CoV}\{X\} = \sqrt{\text{Var}\{X\}}/\mathbb{E}\{X\}$  is the coefficient of variation of a random variable  $X$ .

$\text{CoV}\{R\} = 0$  for a constant rate requirement  $R$ . Therefore, the variance is simplified to

$$\text{Var}\{N\} \cong \mathbb{E}\{N\}\text{CoV}^2\left\{\frac{1}{\eta}\right\}. \quad (12)$$

Since the distribution of  $\bar{N}(W)$  is approximately Gaussian [32, Ch. 7], we now know the approximate distribution of  $N$ . Thus, for example, the number of UEs we can support 97.5% of the time is approximately

$$\mathbb{E}\{N\} - 1.96\sqrt{\text{Var}\{N\}} = \mathbb{E}\{N\} - 1.96\sqrt{\mathbb{E}\{N\}}\text{CoV}\left\{\frac{1}{\eta}\right\}, \quad (13)$$

where 1.96 comes from the Gaussian table for the 97.5% area of the normal distribution.

## B. Site-Level CSO Patterns

We consider 14 different site-level regular CSO patterns, where only entire BSs are switched off (i.e., there is no individual sector switch-off). Most of these patterns appear in the regular CSO patterns literature (see Table I).

The pattern for which all BSs are active (without CSO) is called P(1). Then P( $n/m$ ) is the pattern where  $n$  out of every  $m$  BSs are active; the proportion of active cells in these patterns is  $\rho = \frac{n}{m}$ . For some patterns with the same  $\frac{n}{m}$  there are several distinct rotations. To differentiate between those rotations, patterns are referred to as  $P_X(n/m)$ , where the subscript  $X$  denotes a particular rotation.

Fig. 3 shows the different possible patterns we investigate at the site-level. Those patterns are based on the well-known frequency reuse patterns, where  $m$  is the number of BSs in the reuse cluster. The patterns are assumed to be periodic, i.e., they expand to infinity. However we limited the simulation region, keeping in mind that there should be enough BSs to model all the dominating interferers.

## C. Combining Sector-Level and Site-Level Patterns

Previous papers on regular CSO patterns focus on site-level patterns only, i.e., there is no individual sector switch-off.

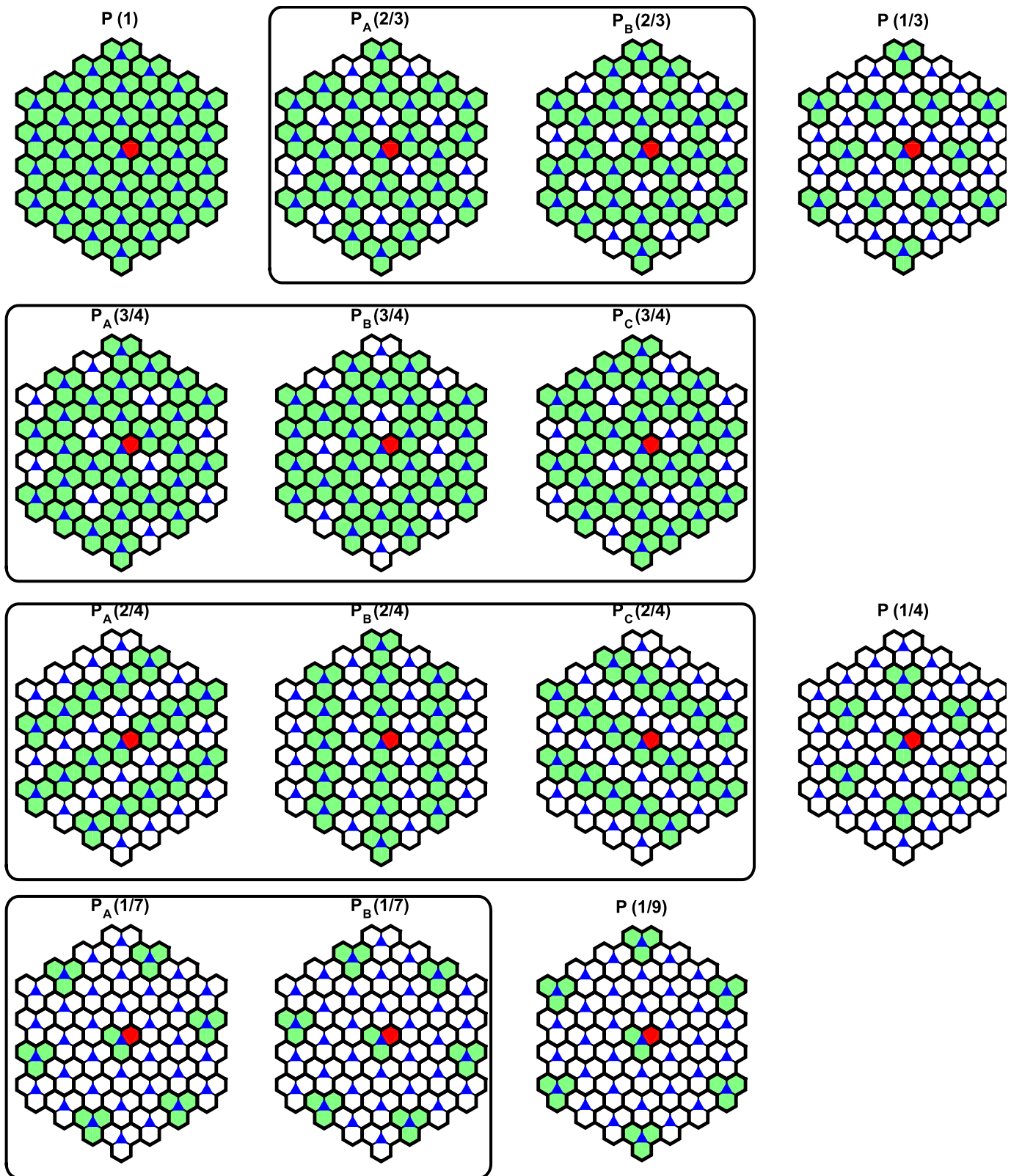


Fig. 3. Site-level patterns: Blue triangles are site locations, each site having three sectors. The red hexagon is sector 1, to which the UE is connected; green hexagons are active sectors which cause interference to the UE; while white hexagons are switched-off sectors. Patterns with the same number of active BSs but having different rotations are enclosed in a rectangle.

For the first time, we investigate the effect of using sector-level regular CSO patterns; these patterns are denoted as  $P(1, k/3)$ , where  $k$  is the number of active sectors per site. The proportion

of active sectors is  $\rho = \frac{k}{3}$ . There are three different patterns at this level: all sectors are active:  $P(1)$ ; two sectors are active:  $P(1, 2/3)$ ; and only one active sector:  $P(1, 1/3)$ . No rotations

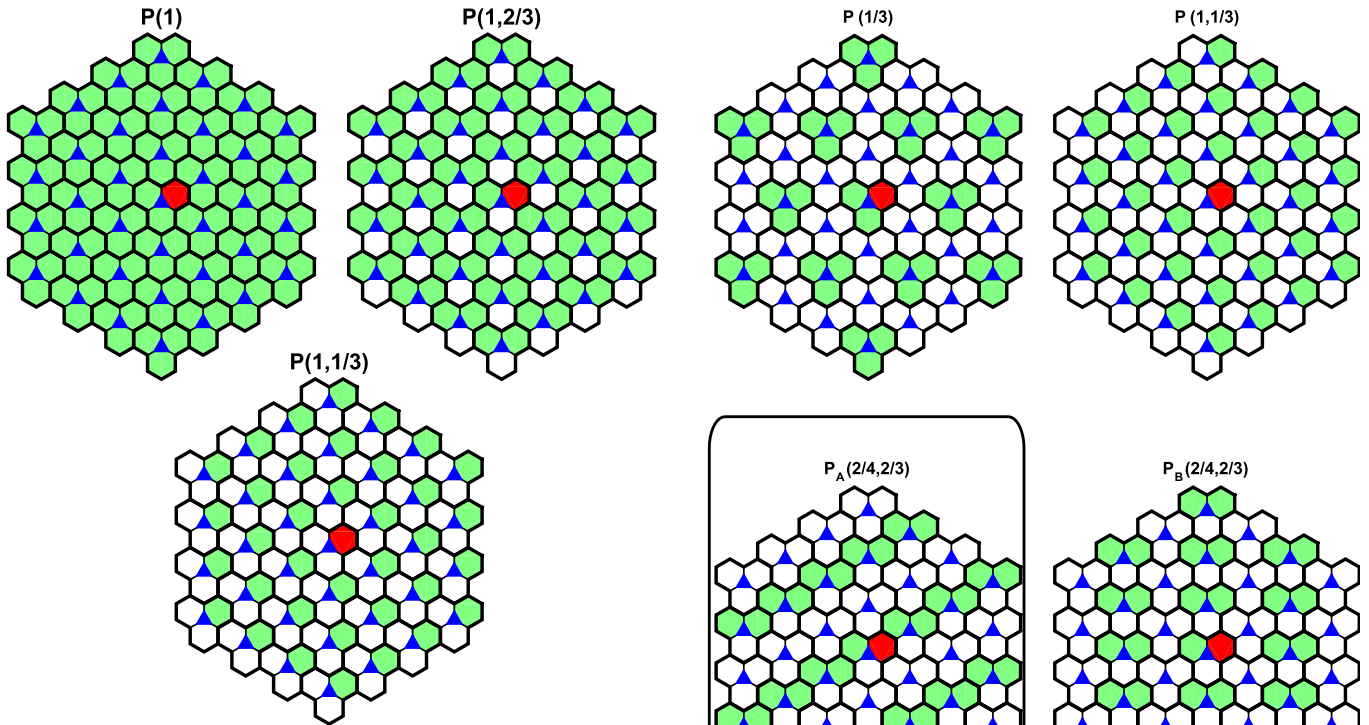


Fig. 4. Sector-level patterns: All BSs are active and only the number of active sectors per BS is different.

are necessary at this level, as site-level patterns already contain all possible rotations. Fig. 4 illustrates the sector-level patterns that can be combined with each site-level pattern to form new patterns.

Sector-level CSO patterns become more interesting when combined with site-level CSO patterns. Any site-level pattern can be combined with any sector-level pattern, in which case the active sectors are those resulting from the logical-AND operation of the two levels of patterns (there are  $14 * 3$  combinations, 26 of them are unique). These patterns are denoted as  $P_X(n/m, k/3)$ , where the subscript  $X$  denotes the rotation of the pattern, the first term inside parenthesis denotes the site-level pattern, and the second term denotes the sector-level pattern. The proportion of active sectors is  $\rho = |P(n/m, k/3)| = \frac{nk}{3m} \in [0, 1]$ .

In order to further illustrate this idea, we focus on two interesting examples. These examples introduce different patterns with the same proportion of active sectors.

1) *One-Third of the Sectors Are Active*: In this example, we illustrate all the CSO patterns where One-third of the sectors are active (i.e.,  $\rho = \frac{1}{3}$ ), namely:  $P(1, 1/3)$ ,  $P(1/3)$ ,  $P_A(2/4, 2/3)$ ,  $P_B(2/4, 2/3)$ , and  $P_C(2/4, 2/3)$ . These patterns are illustrated in Fig. 5. It is worth mentioning that there are different rotations for the case of  $P(2/4, 2/3)$ . Two of them,  $P_A(2/4, 2/3)$  and  $P_B(2/4, 2/3)$ , represent different sectors in the same pattern, whereas  $P_C(2/4, 2/3)$  is a different pattern.

2) *One-Sixth of the Sectors Are Active*: In this example, we illustrate all the CSO patterns where one-sixth of the sectors are active (i.e.,  $\rho = \frac{1}{6}$ ), namely:  $P(1/4, 2/3)$ ,  $P_A(2/4, 1/3)$ ,  $P_B(2/4, 1/3)$  and  $P_C(2/4, 1/3)$ . These patterns

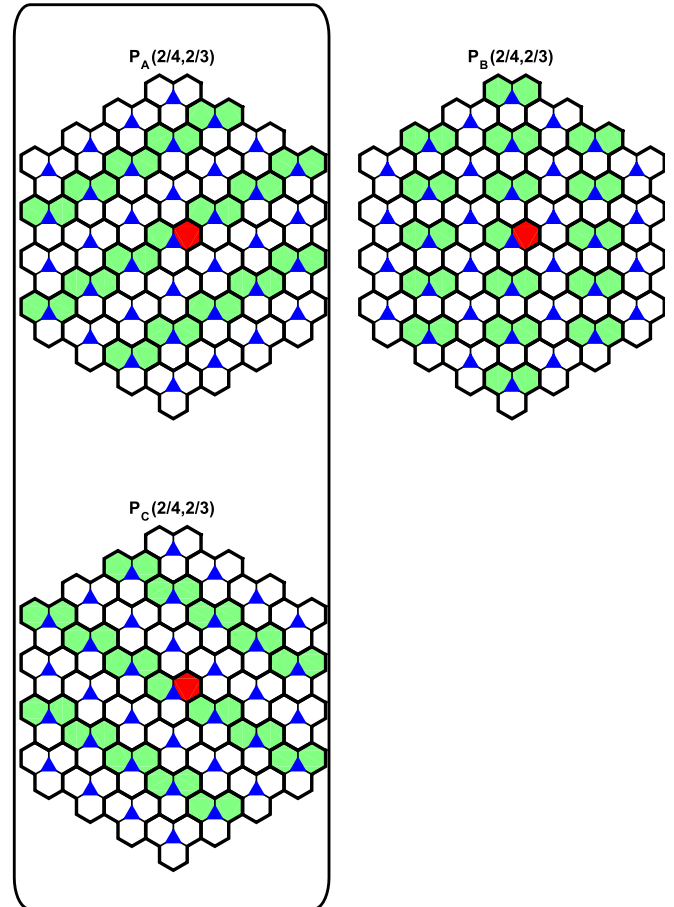


Fig. 5. All patterns with  $\rho = 1/3$ . Patterns inside the rectangle are parts of the same overall pattern.

are illustrated in Fig. 6. It is worth mentioning that there are different rotations for the case of  $P(2/4, 1/3)$ . Two of them,  $P_B(2/4, 1/3)$  and  $P_C(2/4, 1/3)$ , are the same patterns, whereas  $P_A(2/4, 1/3)$  is a different pattern.

We will investigate the first example in detail in Section V.

#### D. Number of Supported Users in the Network

The total number of supported UEs over the total number of sectors in the network is found by multiplying (7) by  $\rho$ :

$$\mathbb{E}\{\rho N\} \cong \frac{W}{\mathbb{E}\{R\}} \eta_{\text{eq}} \rho. \quad (14)$$

In order to find the average number of UEs supported by the network, one simply multiplies (14) by the total number

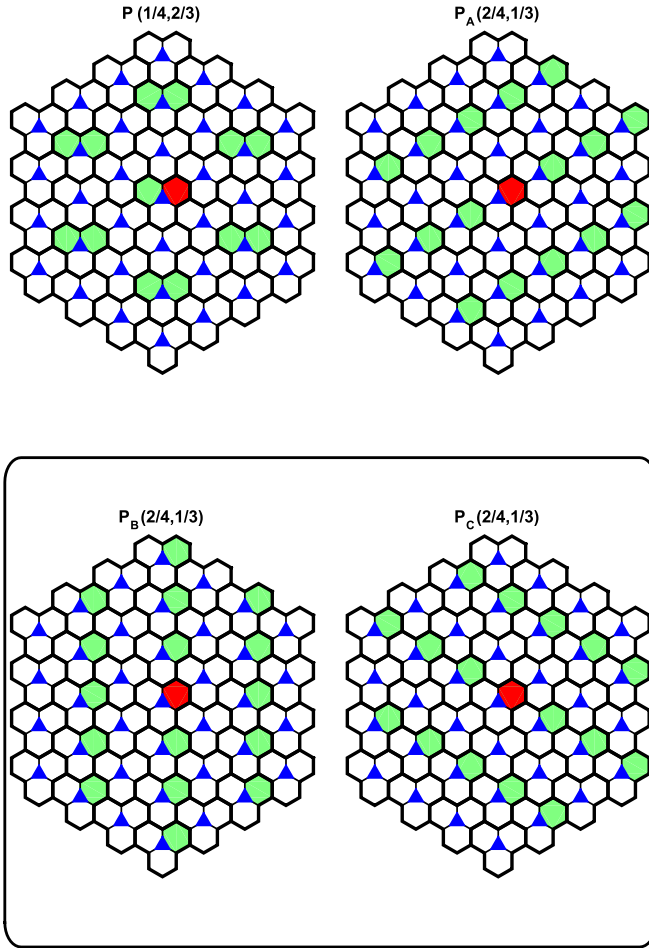


Fig. 6. All patterns with  $\rho = 1/6$ . Patterns inside the rectangle are the same.

of sectors in the network. Thus,  $\eta_{eq} \rho$  is proportional to the average number of UEs supported by the network for a given pattern. Conversely, (14) allows us to choose the CSO pattern that can support a given user density based on  $\eta_{eq} \rho$ .

#### E. Sector-Based vs. Site-Based Energy Efficiency

In some CSO literature, the amount of energy saving is assumed to be directly proportional to the number of switched-off BSs [5], [6], [33]. This is a valid assumption, especially as the power consumption of a BS is highly independent of its load [5], [6]. In a typical LTE network, each BS has three sectors; however, switching off one sector per BS does not necessarily result in one-third of energy saving overall. The fraction of energy saving depends on the common hardware that is shared among the three sectors at each site, such as cooling and baseband processing equipment. This aspect is summarized in Fig. 7. It is necessary to analytically compare site-based versus sector-based CSO patterns in terms of energy efficiency.

The number of active sectors in a CSO pattern is directly proportional to the total energy consumption in the network. Therefore, for two CSO patterns with the same proportion of active sectors, the pattern that can support the most UEs is more energy-efficient. Hence, the power consumption per user is a proper metric for energy-efficiency in this context under

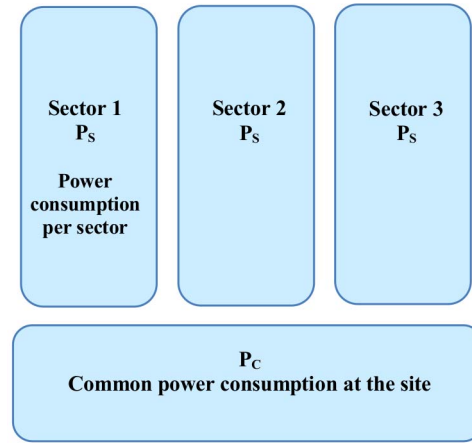


Fig. 7. Power consumption at a site  $P_{site} = P_C + 3P_S$  when all sectors are active.

these assumptions. The average power consumption at each system site of pattern  $P(n/m, k/3)$  is

$$P_{\text{pattern}} = \frac{n}{m}(P_C + kP_S), \quad (15)$$

where  $P_C$  is the common power consumption at the site; and  $P_S$  is the power consumption per sector. This equation is useful to determine which pattern to choose when considering two patterns with the same  $\rho$ .

In this subsection, we provide the analysis to compare the energy efficiency of site-level CSO pattern  $P(n/3m)$ ; with that of the sector-level CSO pattern  $P(n/m, 1/3)$ . Both patterns have the same proportion of active sectors  $\rho = \frac{n}{3m}$ . Then, for pattern  $P(n/m, 1/3)$ , we have

$$P_{\text{pattern},1} = \frac{n}{m}(P_C + 1P_S), \quad (16)$$

and for pattern  $P(n/3m)$ , we have

$$P_{\text{pattern},2} = \frac{n}{3m}(P_C + 3P_S). \quad (17)$$

We compare the energy efficiency in terms of power consumption per user as

$$\frac{P_{\text{pattern},1}}{N_1} = \frac{P_{\text{pattern},2}}{N_2}. \quad (18)$$

The average number of users  $N$  is found from (7) and we substitute in (18) to get

$$\frac{P_{\text{pattern},1}}{\eta_{eq,1}W/\mathbb{E}\{R\}} = \frac{P_{\text{pattern},2}}{\eta_{eq,2}W/\mathbb{E}\{R\}}, \quad (19)$$

which simplifies to

$$\frac{P_{\text{pattern},1}}{P_{\text{pattern},2}} = \frac{\eta_{eq,1}}{\eta_{eq,2}}. \quad (20)$$

Then, substituting (16) and (17) in (20), we obtain

$$\frac{(1 + \alpha)}{(1 + \frac{\alpha}{3})} = \frac{1}{\delta}, \quad (21)$$

where,  $\delta = \eta_{eq,2}/\eta_{eq,1}$  and  $\alpha = P_C/P_S$ .<sup>4</sup>

<sup>4</sup>The value of  $\alpha$  would be known by the network operator.

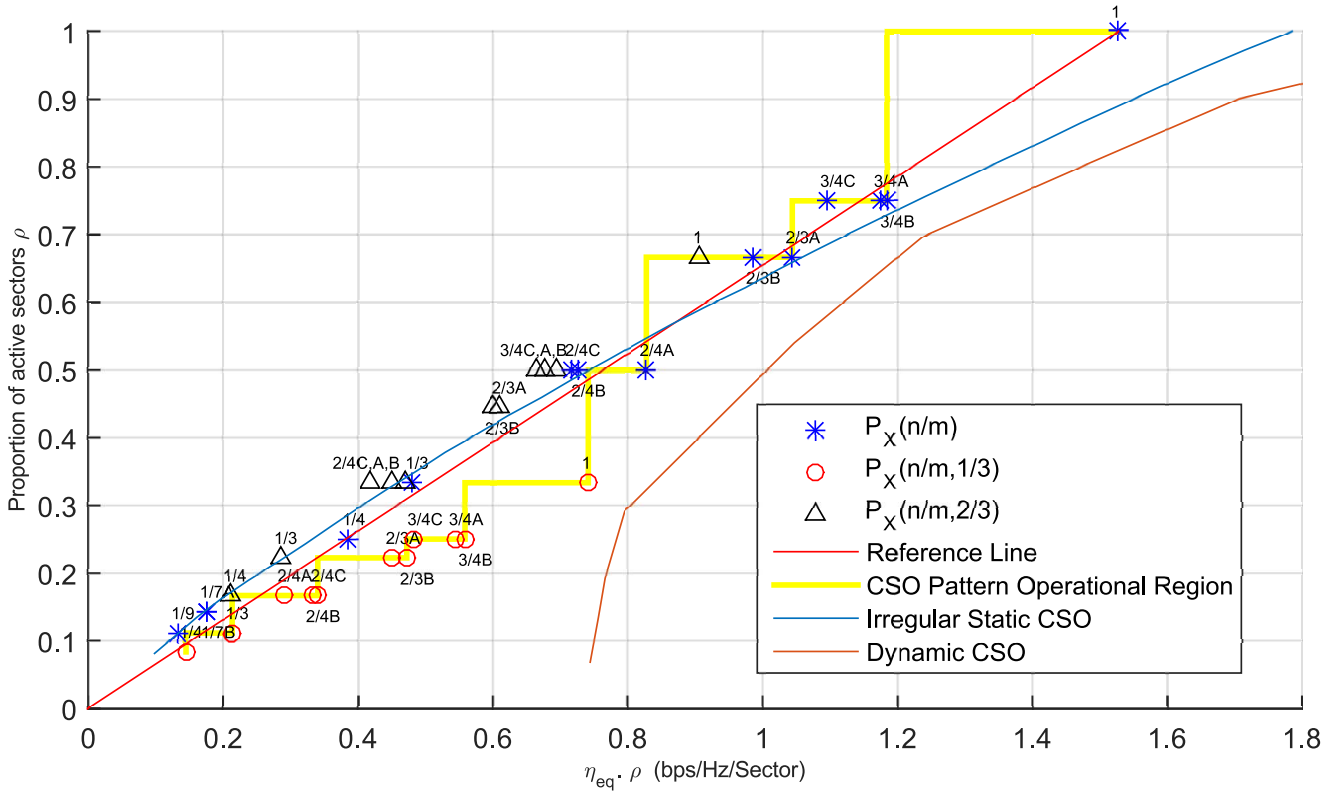


Fig. 8. Performance comparison of different patterns and other CSO schemes for the UMi scenario. The x-axis is proportional to the average number of UEs supported by the network. The y-axis is the proportion of active sectors. The reference line gives locations where the performance of the network is scaled proportionally with respect to the fully active network  $P(1)$ . The operational region curve follows the best performing pattern for any given  $\rho$ . The irregular static CSO is a benchmark from [21], while the dynamic CSO is a benchmark from [16]. Patterns with outage  $P_o > 2\%$  are not included.

Finally, we can find the breakpoint as

$$\alpha^* = \frac{1 - \delta}{\delta - \frac{1}{3}}. \quad (22)$$

If  $\alpha < \alpha^*$  then the site-level pattern  $P(n/3m)$  is more energy efficient; otherwise, the pattern  $P(n/m, 1/3)$  with  $1/3$  active sectors is preferred. Similar calculations can be done for the case of  $2/3$  active sectors; however, we will find in the next section that those patterns are not favourable in terms of energy efficiency, regardless of  $\alpha$ .

#### IV. SIMULATION

In this paper, we consider the downlink of a cellular network with a hexagonal layout. We simulate two ITU scenarios, the Urban Micro-cell (UMi) and the Urban Macro-cell (UMa), according to the evaluation guidelines of [12].

We developed a system-level platform to obtain different statistical values using the simulation parameters listed in Table III. All UEs are uniformly and independently distributed according to a BPP. We then compute the average wide band SINR for all the UEs. We count the number of UEs that experience an SINR level less than  $-7$  dB (the minimum SINR threshold); and calculate the  $P_o$  as the ratio between the number of UEs with insufficient SINR over the total number of UEs. We provide average values of  $P_o$  over 100 realizations. Multipath fading is not considered in the simulation due to the fact that the time-scale of such a phenomenon is often too

TABLE III  
SIMULATION PARAMETERS FOR URBAN MICROCELL (UMi)  
AND URBAN MACROCELL (UMa) SCENARIOS

Parameter	Assumption	
	UMi	UMa
ITU scenario	UMi	UMa
Cellular layout	hexagonal	
Sectorization	three $120^\circ$ sectors	
Maximum forward-to-backward antenna attenuation	20 dB [12, Sec. 8.5]	
Inter-site distance	200 m	500 m
BS antenna height	10 m	25 m
Cell transmit power	41 dBm	46 dBm
Carrier frequency ( $f_c$ )	2.5 GHz	
UE distribution	independent and uniform	
Probability of indoor UEs	0.5	0
UE noise figure	5 dB	
BS noise figure	7 dB	
Thermal noise	-174 dBm/Hz	
Shadowing spread (LOS)	3 dB	4 dB
Shadowing spread (NLOS)	4 dB	6 dB
SINR range	[-7, 18] dB	
Traffic type	full queue	

short for the CSO implementation. Sector 1 (the red hexagon in Fig. 3) is chosen as a typical sector; we consider all UEs that get the best downlink SINR when connected to sector 1. Other active sectors (green hexagons) will cause interference to those UEs.

We considered a rather simple resource allocation scheme as follows: each user is assigned a portion of the bandwidth

TABLE IV  
CHARACTERISTIC VALUES OF CSO PATTERNS

Pattern	UMi				UMa			
	$\eta_{eq}$	$\eta_{eq}\cdot\rho$	$P_o\%$	$CoV\left\{\frac{1}{\eta}\right\}$	$\eta_{eq}$	$\eta_{eq}\cdot\rho$	$P_o\%$	$CoV\left\{\frac{1}{\eta}\right\}$
P(1)	1.53	1.53	0.00	0.75	1.37	1.37	0.00	0.63
P(1, 2/3)	1.36	0.91	0.10	0.75	1.36	0.91	0.00	0.66
P(1, 1/3)	2.22	0.74	0.00	0.82	2.06	0.69	0.08	0.86
P <sub>A</sub> (2/3) P <sub>B</sub> (2/3)	1.53	1.02	0.00	0.75	1.32	0.88	0.05	0.70
P <sub>A</sub> (2/3, 2/3) P <sub>B</sub> (2/3, 2/3)	1.36	0.61	0.057	0.73	1.31	0.59	0.07	0.73
P <sub>A</sub> (2/3, 1/3) P <sub>B</sub> (2/3, 1/3)	2.08	0.46	0.01	0.94	1.72	0.39	0.67	0.95
P(1/3)	1.44	0.48	0.76	0.84	1.36	0.45	0.82	0.83
P(1/3, 2/3)	1.28	0.29	0.15	0.78	1.17	0.26	1.35	0.80
P(1/3, 1/3)	1.92	0.21	0.14	0.95	1.48	0.16	3.41	0.97
P <sub>A</sub> (3/4) P <sub>B</sub> (3/4) P <sub>C</sub> (3/4)	1.54	1.15	0.01	0.74	1.33	1.0	0.07	0.69
P <sub>A</sub> (3/4, 2/3) P <sub>B</sub> (3/4, 2/3) P <sub>C</sub> (3/4, 2/3)	1.36	0.68	0.05	0.74	1.31	0.66	0.09	0.72
P <sub>A</sub> (3/4, 1/3) P <sub>B</sub> (3/4, 1/3) P <sub>C</sub> (3/4, 1/3)	2.14	0.55	0.01	0.91	0.78	0.44	0.46	0.95
P <sub>A</sub> (2/4) P <sub>B</sub> (2/4) P <sub>C</sub> (2/4)	1.51	0.76	0.01	1.75	1.35	1.67	0.08	1.71
P <sub>A</sub> (2/4, 2/3) P <sub>C</sub> (2/4, 2/3)	1.30	0.44	0.08	0.74	1.18	0.40	0.75	0.76
P <sub>B</sub> (2/4, 2/3)	1.41	0.47	0.01	0.73	1.42	0.47	0.09	0.75
P <sub>A</sub> (2/4, 1/3)	1.75	0.29	0.30	1.03	1.36	0.23	2.64	0.97
P <sub>B</sub> (2/4, 1/3) P <sub>C</sub> (2/4, 1/3)	2.02	0.34	0.01	0.90	1.63	0.27	1.29	0.96
P(1/4)	1.55	0.39	0.00	0.69	1.45	0.36	0.39	0.75
P(1/4, 2/3)	1.26	0.21	0.35	0.76	1.14	0.19	2.80	0.83
P(1/4, 1/3)	1.74	0.14	0.54	0.98	1.42	0.12	5.66	0.98
P <sub>A</sub> (1/7) P <sub>B</sub> (1/7)	1.24	0.18	0.84	0.77	1.15	0.17	5.82	0.82
P <sub>A</sub> (1/7, 2/3) P <sub>B</sub> (1/7, 2/3)	1.08	0.10	2.63	0.78	1.05	0.10	9.57	0.81
P <sub>A</sub> (1/7, 1/3) P <sub>B</sub> (1/7, 1/3)	1.46	0.07	4.66	1.05	1.37	0.07	14.45	1.03
P(1/9)	1.20	0.13	1.21	0.78	1.16	0.13	8.53	0.84
P(1/9, 2/3)	1.08	0.08	4.65	0.79	1.04	0.08	13.26	0.82
P(1/9, 1/3)	1.41	0.05	8.46	1.06	1.32	0.05	18.68	1.01

based on its spectral efficiency such that its required rate is satisfied. Although this resource allocation scheme might be conservative (in terms of aggregate rate) compared to a more sophisticated power/time/frequency allocations, it allows it allows to carry out a meaningful performance assessment and fair comparative study; thus, leading to valid and general conclusions.

For each CSO pattern, we drop a large number of UEs to estimate the ESE according to (8), as well as  $P_o$  and  $CoV\{1/\eta\}$ . Results are summarized in Table IV for both the UMi and the UMa scenarios. From this table we conclude that some patterns will cause a high probability of outage, therefore they are not included in Fig. 8. The metric  $\eta_{eq}\cdot\rho$  – equivalent spectral efficiency per sector – is shown in the third column. Using this metric, we visually compared the performance of different CSO patterns in Fig. 8.

Fig. 8 compares the performance of different CSO patterns. The x-axis is proportional to the average number of UEs that can be supported by the network, as given by (14), and hence is also proportional to the aggregate rate. The y-axis is the

proportion of active sectors  $\rho$ . The energy consumption of the network when configured to a particular pattern is computed from both  $\rho$  and the marker type; different markers indicate the number of active sectors per BS site. The reference line indicates where the performance of the network is scaled proportionally with respect to the fully active network P(1). The trend is that patterns with all sectors active fall close to the reference line, while patterns with two active sectors per BS fall to the left of the reference line (i.e., perform worse). Interestingly, patterns with one active sector per BS fall to the right of the line (i.e., perform better). Notably, consider the case of  $\rho = 1/3$ : the number of active sectors is reduced to one-third; however, the average number of UEs that can be supported by pattern P(1, 1/3) is only reduced to 48.5%. This means that almost half of full capacity is achieved using only 1/3 of the sectors. The yellow staircase curve shows the operational region based on the best performing pattern for any given  $\rho$ . This curve represents the temporal domain of the CSO patterns (i.e., when to apply a different pattern), and can be used by operators to select the best pattern that can support

a given user density demand.<sup>5</sup> The operational region (yellow staircase), could be used directly only for the specific case of  $\alpha = 0$  (no common power).

In order to make the study complete, we compare the performance of the proposed regular CSO patterns with two benchmark algorithms from irregular static (offline) CSO [21, Algorithm 1] and dynamic (online) CSO [16, Algorithm 1]. Note that the values for irregular static CSO are obtained according to the simulation parameters indicated in [21], but with a uniform UE distribution. As we can conclude from the figure, regular CSO patterns perform comparably and even better at some points, to the irregular static CSO. For the case of dynamic CSO, the values in the curve are obtained according to the simulation parameters indicated in [16], but with a uniform UE distribution. It is worth mentioning that the simulation parameters used in [16] are not entirely compliant with our simulation parameters. One fundamental difference is that in [16], UEs are served in a way that maximizes the aggregate network capacity, i.e., UEs with high spectral efficiency are provided with large bandwidth, while UEs with low spectral efficiency might be blocked. In contrast, in our simulation, UEs are admitted on a first-come, first-served basis.

## V. CASE STUDY

In this section, we further investigate all the CSO patterns with  $\rho = 1/3$ , shown in Fig. 5 (the first example from Section III-C). All the figures in this section are for the UMi scenario; however, we find that the UMa scenario results in a similar trend [1].

### A. SINR Distribution

Each CSO pattern results in a different spatial distribution of the SINR of a typical UE conditioned to be connected to sector 1, as seen in Fig. 9.

Fig. 10 shows the effect of the chosen patterns on the resulting cumulative distribution function (CDF) of the downlink SINR for UEs connected to sector 1. To validate our simulation platform, we also included the average CDF results obtained from the WINNER+ project using multiple simulation tools [30]. As shown in the figure, the SINRs obtained from pattern P(1) have a CDF that closely matches the WINNER+ results. Note that pattern P(1) is the case where all cells are active, i.e., without CSO.

It is worth mentioning that there is a high improvement in the SINR in pattern P(1, 1/3), where only one sector is active per site. This improvement is due to the significant reduction in the number of nearby interferers. Moreover, the SINR values are truncated at 18 dB [31]; higher SINR values might be of interest in future systems that allow for higher constellations.

### B. Number of Users Per Sector

We now compare the number of supported UEs per active sector for all patterns with  $\rho = 1/3$ . After finding  $\eta_{eq}$  and

<sup>5</sup>Operators can use this curve as an enabler for automatic switching between CSO patterns as the traffic load evolves throughout the day.

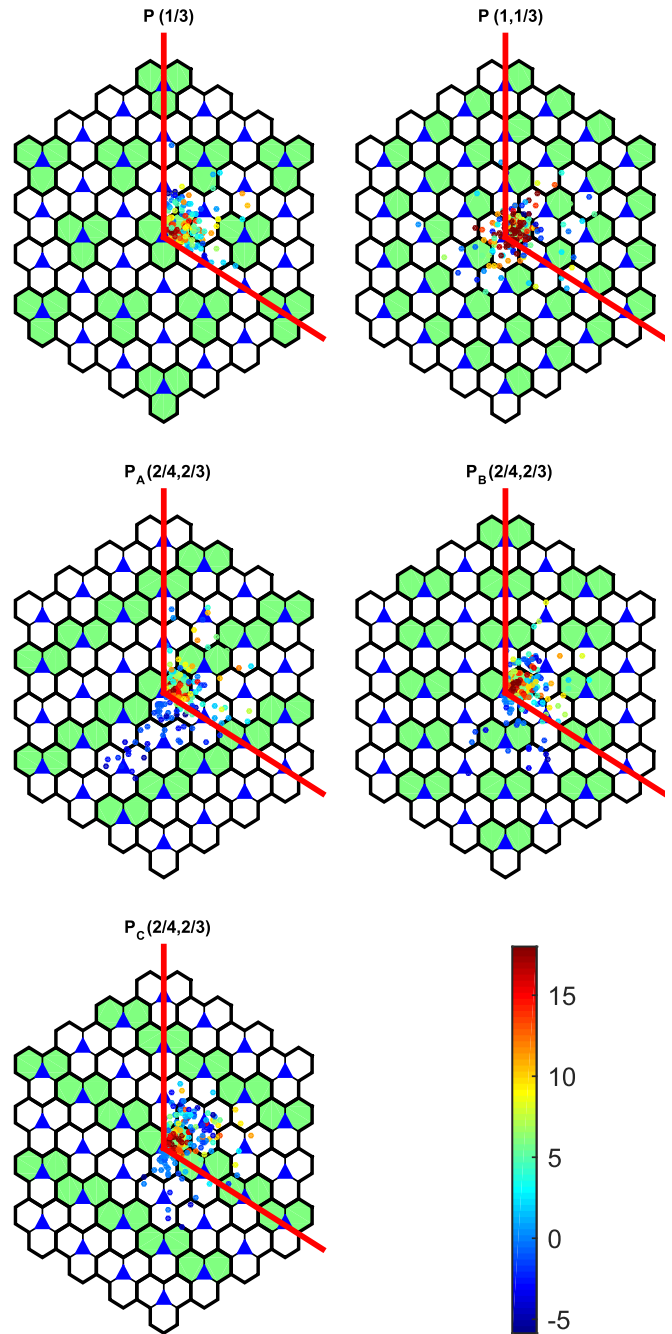


Fig. 9. Conditional spatial distribution of the SINR (in dB) of a typical UE when connected to sector 1, for patterns in Fig. 5, for the UMi scenario (the UMa scenario shows a similar trend). The UE is connected to the sector that results in the highest downlink SINR.

CoV  $\{1/\eta\}$  for each pattern, we assume a constant rate demand of 500 kbps and a system bandwidth of 10 MHz, resulting in  $W/\mathbb{E}\{R\} = 20$  and  $\text{CoV}\{R\} = 0$ . We also find the number of UEs that a typical sector can support, and show both the simulated and the closely matching analytical CDFs (from Section III-A2) in Fig. 11. Analytical calculations show that the P(1, 1/3) pattern can support the most UEs (44.5 UEs) per sector on average - this is also approximately the median (50%), since  $N$  is close to Gaussian- and about 33 UEs 97.5% of the time (according to (13)). The distribution

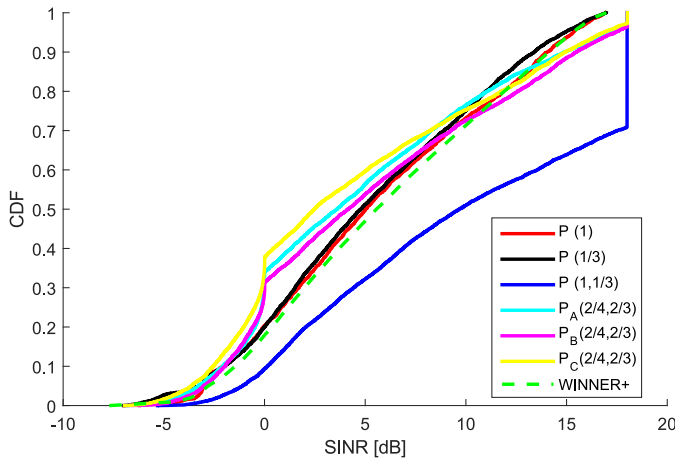


Fig. 10. CDFs of SINR for patterns in Fig. 5 for the UMi scenario, with WINNER+ [30] calibration for the fully active network (pattern P(1)). Interestingly, patterns with 2 out of 3 sectors active per BS have a large number of UEs with SINR around 0 dB; this is due to the spatial geometry of these patterns (see Fig. 8 for visualizations of the SINR coverage maps).

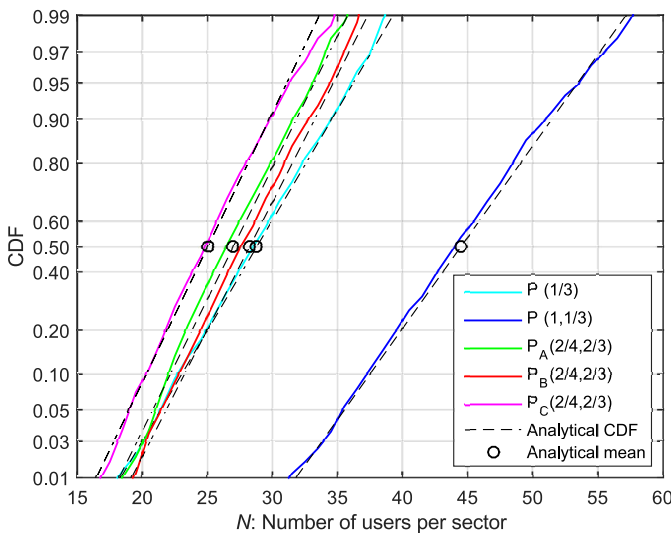


Fig. 11. CDFs of the number  $N$  of UEs supported for patterns in Fig. 5, when  $R$  is constant and  $W/R = 20$ , for the UMi scenario. The y-axis is transformed so that all and only Gaussian distributions appear as straight lines. The coloured curves are simulated CDFs, which closely match the analytical CDFs. Black circles are the analytical means, which are close to the simulation medians (50%).

of the number of UEs closely follows a Gaussian distribution, as expected from the analysis in Section III-A2.

### C. Energy Efficiency Aspects

Based on the calculations in Section III-E, we can find the breakpoint that indicates which pattern is better in terms of energy efficiency per UE. While the patterns with 2/3 active sectors are never advantageous, the pattern P(1, 1/3) is advantageous over pattern P(1/3), as long as  $P_C/P_S > \alpha = 1.114$ , as found from (22).

## VI. CONCLUSION

CSO is a promising approach for more energy-efficient cellular networks. In this paper, we classified the CSO approaches, investigated 26 different regular CSO patterns in

detail, and presented them using a systematic nomenclature. Furthermore, this paper was the first to investigate sector-based regular CSO patterns. The performances of different CSO patterns were compared using only one parameter. The distribution of the number of users supported was found to be close to Gaussian with a variance estimated using one additional parameter. The maximum number of supported users was usually obtained from patterns where one sector out of three is active at a site. In many cases, the performance of regular CSO patterns is comparable to that of a benchmark irregular static CSO. Moreover, although a benchmark dynamic CSO outperforms the regular CSO patterns, it is still reasonable to employ the regular CSO patterns because of their simplicity and scalability.

The next, nontrivial step is to investigate CSO configurations using a sophisticated resource allocation scheme in the presence of a spatially-irregular BS deployment for any given demand distribution. Since the combinatorial search space of the problem of switching off  $n$  out of  $m$  cells explodes exponentially for even a moderate number of BSs, therefore, it is very useful to have good starting heuristics for the choice of selected BSs/sectors (e.g., the initial population for a genetic algorithm [10]), which can later be refined. As such, our work can be an intermediate step in studying CSO under more realistic (irregular BS locations and/or non-uniform demand distributions) assumptions. Also, CSO patterns can be combined with online CSO algorithms to form a hybrid approach that can accommodate non-uniform demand distributions. Moreover, if the demand distribution is non-uniform over a large area, but still relatively uniform along smaller areas, different regular CSO patterns could still be used on the different smaller areas (perhaps with some modifications needed at the borders).

Regular CSO patterns are conceptually simple and can be characterized systematically both statistically and geometrically. Location regularity of CSO patterns provides the advantages of: 1) ensuring that interferer cells are as far away as possible, 2) allowing for realistic interference modelling, 3) minimizing the coverage holes, and 4) being more energy-efficient for users in the uplink transmission, since users do not need to transmit at full power because there is always a nearby active cell.

## REFERENCES

- [1] T. Beitelmal, S. S. Szyszkowicz, and H. Yanikomeroglu, "Regular and static sector-based cell switch-off patterns," in *Proc. IEEE Veh. Technol. Conf. (VTC-Fall)*, Sep. 2016, pp. 1–5.
- [2] J. G. Andrews *et al.*, "What will 5G be?" *IEEE J. Sel. Areas Commun.*, vol. 32, no. 6, pp. 1065–1082, Jun. 2014.
- [3] Z. Hasan, H. Boostanimehr, and V. K. Bhargava, "Green cellular networks: A survey, some research issues and challenges," *IEEE Commun. Surveys Tuts.*, vol. 13, no. 4, pp. 524–540, 4th Quart., 2011.
- [4] I. Humar, X. Ge, L. Xiang, M. Jo, M. Chen, and J. Zhang, "Rethinking energy efficiency models of cellular networks with embodied energy," *IEEE Netw.*, vol. 25, no. 2, pp. 40–49, Mar./Apr. 2011.
- [5] T. Beitelmal and H. Yanikomeroglu, "A set cover based algorithm for cell switch-off with different cell sorting criteria," in *Proc. IEEE Int. Conf. Commun. Workshops (ICC Workshops)*, Jun. 2014, pp. 641–646.
- [6] D. González G., H. Yanikomeroglu, M. Garcia-Lozano, and S. R. Boque, "A novel multiobjective framework for cell switch-off in dense cellular networks," in *Proc. IEEE Int. Conf. Commun. (ICC)*, Jun. 2014, pp. 2641–2647.

- [7] L. Budzisz *et al.*, "Dynamic resource provisioning for energy efficiency in wireless access networks: A survey and an outlook," *IEEE Commun. Surveys Tuts.*, vol. 16, no. 4, pp. 2259–2285, 4th Quart., 2014.
- [8] K. C. Tun and K. Kunavut, "An overview of cell zooming algorithms and power saving capabilities in wireless networks," *Int. J. Appl. Sci. Technol.*, vol. 7, no. 3, pp. 1–13, Jul. 2014.
- [9] Z. Niu, Y. Wu, J. Gong, and Z. Yang, "Cell zooming for cost-efficient green cellular networks," *IEEE Commun. Mag.*, vol. 48, no. 11, pp. 74–79, Nov. 2010.
- [10] F. Alaca, A. Bin Sediq, and H. Yanikomeroglu, "A genetic algorithm based cell switch-off scheme for energy saving in dense cell deployments," in *Proc. IEEE Global Commun. Conf. Workshops (GLOBECOM Workshops)*, Dec. 2012, pp. 63–68.
- [11] A. Guo and M. Haenggi, "Spatial stochastic models and metrics for the structure of base stations in cellular networks," *IEEE Trans. Wireless Commun.*, vol. 12, no. 11, pp. 5800–5812, Nov. 2013.
- [12] *Guidelines for Evaluation of Radio Interface Technologies for IMT-Advanced*, document ITU-R M.2135-1, ITU-R, 2009.
- [13] F. Lagum, Q.-N. Le-The, T. Beitelmal, S. S. Szyszkowicz, and H. Yanikomeroglu, "Cell switch-off for networks deployed with variable spatial regularity," *IEEE Wireless Commun. Lett.*, vol. 6, no. 2, pp. 234–237, Apr. 2017.
- [14] Q.-N. Le-The, T. Beitelmal, F. Lagum, S. S. Szyszkowicz, and H. Yanikomeroglu, "Cell switch-off algorithms for spatially irregular base station deployments," *IEEE Wireless Commun. Lett.*, vol. 6, no. 3, pp. 354–357, Jun. 2017.
- [15] M. A. Marsan, L. Chiaraviglio, D. Ciullo, and M. Meo, "Switch-off transients in cellular access networks with sleep modes," in *Proc. IEEE Int. Conf. Commun. Workshops (ICC Workshops)*, Jun. 2011, pp. 1–6.
- [16] A. S. Alam, L. S. Dooley, and A. S. Poulton, "Traffic-and-interference aware base station switching for green cellular networks," in *Proc. IEEE Int. Workshop Comput. Aided Modeling Design Commun. Links Netw. (CAMAD)*, Sep. 2013, pp. 63–67.
- [17] S. Kokkinogonis and G. Koutitas, "Dynamic and static base station management schemes for cellular networks," in *Proc. IEEE Global Commun. Conf. (GLOBECOM)*, Dec. 2012, pp. 1–6.
- [18] A. K. M. F. Haque, A. F. M. S. Shah, M. A. Hannan, N. Jahan, U. Ahmed, and A. Saleh, "High performance analysis of frequency reuse schemes in cellular mobile environment," *Int. J. Latest Trends Comput.*, vol. 2, no. 1, pp. 29–34, Mar. 2011.
- [19] M. A. Marsan, L. Chiaraviglio, D. Ciullo, and M. Meo, "Optimal energy savings in cellular access networks," in *Proc. IEEE Int. Conf. Commun. Workshops (ICC Workshops)*, Jun. 2009, pp. 1–5.
- [20] F. Han, Z. Safar, W. Lin, Y. Chen, and K. J. R. Liu, "Energy-efficient cellular network operation via base station cooperation," in *Proc. IEEE Int. Conf. Commun. (ICC)*, Jun. 2012, pp. 4374–4378.
- [21] D. González G., J. Hämäläinen, H. Yanikomeroglu, M. García-Lozano, and G. Senarath, "A novel multiobjective cell switch-off framework for cellular networks," *IEEE Access*, vol. 4, pp. 7883–7898, Nov. 2016.
- [22] L. Suárez, L. Nuaymi, and J.-M. Bonnin, "Energy-efficient BS switching-off and cell topology management for macro/femto environments," *Comput. Netw.*, vol. 78, pp. 182–201, Feb. 2014.
- [23] I. Aydın, H. Yanikomeroglu, and U. Aygolu, "User-aware cell switch-off algorithms," in *Proc. Int. Wireless Commun. Mobile Comput. Conf. (IWCMC)*, Aug. 2015, pp. 1236–1241.
- [24] L. Chiaraviglio, D. Ciullo, M. Meo, and M. A. Marsan, "Energy-efficient management of UMTS access networks," in *Proc. IEEE Congr. Teletraffic (ITC)*, Sep. 2009, pp. 1–8.
- [25] X. Weng, D. Cao, and Z. Niu, "Energy-efficient cellular network planning under insufficient cell zooming," in *Proc. IEEE Veh. Technol. Conf. (VTC-Spring)*, May 2011, pp. 1–5.
- [26] L. B. Le, "QoS-aware BS switching and cell zooming design for OFDMA green cellular networks," in *Proc. IEEE Global Commun. Conf. (GLOBECOM)*, Dec. 2012, pp. 1544–1549.
- [27] A. Kumar and C. Rosenberg, "Energy and throughput trade-offs in cellular networks using base station switching," *IEEE Trans. Mobile Comput.*, vol. 15, no. 2, pp. 364–376, Feb. 2016.
- [28] *Telecommunication Management; Study on Energy Savings Management (ESM)*, document TR 32.826, 3rd Generation Partnership Project, Apr. 2010.
- [29] X. Guo, Z. Niu, S. Zhou, and P. R. Kumar, "Delay-constrained energy-optimal base station sleeping control," *IEEE J. Sel. Areas Commun.*, vol. 34, no. 5, pp. 1073–1085, May 2016.
- [30] *Calibration for IMT-Advanced Evaluations*, document CELTIC/CP5-026 Project WINNER+, Munich, Germany, May 2010.
- [31] D. Bultmann, T. Andre, and R. Schoenen, "Analysis of 3GPP LTE-Advanced cell spectral efficiency," in *Proc. IEEE Int. Symp. Pers. Indoor Mobile Radio Commun. (PIMRC)*, Sep. 2010, pp. 1876–1881.
- [32] S. M. Ross, *Introduction to Probability Models*. Burlington, MA, USA: Academic Press, 2010.
- [33] H. Holtkamp, G. Auer, V. Giannini, and H. Haas, "A parameterized base station power model," *IEEE Commun. Lett.*, vol. 17, no. 11, pp. 2033–2035, Nov. 2013.



**Tamer Beitelmal** received the B.Sc. and M.Sc. degrees in electrical and electronics engineering from Garyounis University, Benghazi, Libya, in 2001 and 2008, respectively, and the Ph.D. degree in electrical and computer engineering from Carleton University, Ottawa, Canada, in 2016. His Ph.D. thesis was the cell switch-off approach for energy efficient cellular networks. His Ph.D. degree was sponsored in part by the Libyan Government through the Ministry of Higher Education and Scientific Research and in part by the Ontario Graduate Scholarships.

**Sebastian S. Szyszkowicz** (S'06–M'11) received the B.A.Sc. degree in electrical engineering (specializing in communications) from the University of Ottawa, ON, Canada, in 2003, and the M.A.Sc. and Ph.D. degrees in electrical and computer engineering from Carleton University, Ottawa, in 2007 and 2011, respectively. In 2008, he was a Visiting Researcher with the University of Edinburgh, Edinburgh, U.K., and he has given several invited talks about the Ph.D. research at universities in Europe and Canada. From 2011 to 2012, he was a Visiting Fellow with the Communications Research Centre, Canada. Since 2016, he has been an Adjunct Research Professor with Carleton University. In 2017, he received the NSERC Discovery Grant for five years. His research focuses on outdoor urban channel modeling: line-of-sight probability, pathloss, mm-wave, spatially correlated shadowing; stochastic geometry for modeling base station and user locations; and green communications: cell switch-OFF. He was a recipient of research awards from the Natural Sciences and Engineering Research Council of Canada: Postgraduate Scholarships at both the master's and the Ph.D. levels, and a Visiting Fellowship and a Post-Doctoral Fellowship at the postdoctoral level.



**David González G.** (S'06–M'15) was born in Chitré, Panamá. He received the B.S. degree in electronics and communications engineering from Universidad de Panamá in 2002, and the master's and Ph.D. degrees from the Universitat Politècnica de Catalunya, Spain, in 2008 and 2013, respectively. From 2002 to 2005, he was a Telecommunication Engineer at Cable Onda, a cable TV operator in Panamá, where he was involved in the integration of digital telephony services. During this period, he also served as a Lecturer with the Universidad Tecnológica de Panamá. In 2014, he joined the Department of Communications and Networking with Aalto University, Finland. His current research activities are focused on the diverse aspects of cellular networks and wireless communications, including interference modeling/coordination, radio access modeling/optimization, and 5G standardization.



**Halim Yanikomeroglu** (F'17) was born in Giresun, Turkey, in 1968. He received the B.Sc. degree in electrical and electronics engineering from Middle East Technical University, Ankara, Turkey, and the M.A.Sc. degree in electrical engineering (now ECE) and the Ph.D. degree in electrical and computer engineering from the University of Toronto, Toronto, ON, Canada, in 1990, 1992, and 1998, respectively. From 1993 to 1994, he was with the Research and Development Group of Marconi Kominikasyon A.S., Ankara. Since 1998, he has been with the

Department of Systems and Computer Engineering, Carleton University, Ottawa, ON, where he is currently a Full Professor. From 2011 to 2012, he was with the TOBB University of Economics and Technology, Ankara, as a Visiting Professor. He is also a registered professional engineer in ON, Canada. In recent years, his research has been funded by Huawei, Telus, Allen Vanguard, Mapsted, Blackberry, Samsung, the Communications Research Centre of Canada, and DragonWave. This collaborative research resulted in over 30 patents (granted and applied). His research interests include wireless

technologies with a special emphasis on wireless networks including the non-terrestrial networks. He was a recipient of the IEEE Ottawa Section Outstanding Educator Award in 2014, Carleton University Faculty Graduate Mentoring Award in 2010, the Carleton University Graduate Students Association Excellence Award in Graduate Teaching in 2010, and the Carleton University Research Achievement Award in 2009 and 2018. He has been involved in the organization of the IEEE Wireless Communications and Networking Conference (WCNC) from its inception, including serving as a Steering Committee Member and a Technical Program Chair or Co-Chair of WCNC 2004, Atlanta, GA, USA, WCNC 2008, Las Vegas, NV, USA, and WCNC 2014, Istanbul, Turkey. He was the General Co-Chair of the IEEE Vehicular Technology Conference (VTC) 2010-Fall, Ottawa, and the General Chair of IEEE VTC 2017-Fall, Toronto. He was the Chair of the IEEE Wireless Technical Committee. He is a Distinguished Lecturer for the IEEE Communications Society and a Distinguished Speaker for the IEEE Vehicular Technology Society. He has served on the Editorial Boards for the IEEE TRANSACTIONS ON COMMUNICATIONS, the IEEE TRANSACTIONS ON WIRELESS COMMUNICATIONS, and the IEEE COMMUNICATIONS SURVEYS AND TUTORIALS.